Surface Plasmon Characteristics of Tunable Photoluminescence in Single Gold Nanorods

A. Bouhelier,[1] R. Bachelot,[2] G. Lerondel,[2] S. Kostcheev,[2] P. Royer,[2] and G. P. Wiederrecht[1]

[1]*Chemistry Division and Center for Nanoscale Materials, Argonne National Laboratory, Argonne, Illinois 60439, USA*

[2]*Laboratoire de Nanotechnologie et d'Instrumentation Optique, Université de Technologie de Troyes, CNRS-FRE 2671, 10010 Troyes, France*

(Received 5 August 2005; published 23 December 2005)

Light emission resulting from two-photon excited gold nanoparticles has been proposed to originate from the radiative decay of surface plasmon resonances. In this vein, we investigated luminescence from individual gold nanorods and found that their emission characteristics closely resemble surface plasmon behavior. In particular, we observed spectral similarities between the scattering spectra of individual nanorods and their photoluminescence emission. We also measured a blueshift of the photoluminescence peak wavelength with decreasing aspect ratio of the nanorods as well as an optically tunable shape-dependent spectrum of the photoluminescence. The emission yield of single nanorods strongly depends on the orientation of the incident polarization consistent with the properties of surface plasmons.

DOI: 10.1103/PhysRevLett.95.267405 PACS numbers: 78.67.Bf, 73.20.Mf, 73.22.−f, 78.55.−m

Local surface plasmons resonances are widely accepted to be the basis for improving the efficiency of absorption and emission processes through a local electromagnetic field enhancement. Nonlinear processes on gold surfaces such as second harmonic generation [1] or two-photon induced photoluminescence (TPPL) [2] are particularly sensitive to these resonances due to their quadratic dependence on the intensity. Isolated regions of enhanced photoluminescence yield on rough gold surfaces were identified through confocal and near-field microscopy [3,4] emphasizing the physical similarities with surface enhanced Raman scattering (SERS) substrates [5]. Gold photoluminescence [6] excited by a multiphoton process has received an increased interest recently for its potential applications in photostable biological labeling [7], characterization of plasmonic modes in nanostructures [8,9], and tailoring light emission through nanoscale optical antennas [10,11]. In recent studies, multiphoton absorption of gold nanostructures has even been shown to produce local near-field enhancement large enough to induce supercontinuum generation in the surrounding environment [11].

Two-photon induced photoluminescence in gold is generally considered as a three-step process. Electrons from occupied d bands are first excited by two-photon absorption to unoccupied states of the sp-conduction band. Second, subsequent intraband scattering processes move the electrons closer to the Fermi level. Third, the relaxation of the electron-hole pair recombines either through nonradiative processes or by emission of luminescence. Radiative relaxation energies are therefore strongly connected to the interband separation, and for bulk material these energies occur around the X and L points of the Brillouin zone [12]. For the case of small particles where the optical properties are dominated by localized surface plasmon resonances, photoluminescence spectra are observed at the same energy as extinction and scattering spectra [3,13,14], suggesting that the photoemission is related to the particle plasmons.

In this Letter, we show that the photoluminescence of gold nanorods excited by a two-photon process presents optical characteristics similar to that of a radiative surface plasmon. Gold nanorods provide an ideal test sample to verify the influence of surface plasmons in the spectral content of the photoemission. Nanorods are characterized by two spectral resonances corresponding to electron oscillations along the longitudinal and the transverse dimensions and are therefore sensitive to both excitation energy and polarization.

We fabricated isolated 45 nm thick gold nanorods by standard electron-beam lithography. The longitudinal axes of the rods were varied from 300 nm down to 50 nm, while keeping the transverse dimension fixed at 30 nm resulting in aspect ratios r of 10, 5, 3.3, 2.3, and 1.6, respectively. The experimental apparatus consisted of a mode-locked Ti:sapphire laser producing 120 fs pulses at an excitation wavelength λ of 785 nm. The laser beam was linearly polarized and directed into a confocal microscope equipped with a 1.4 numerical aperture objective. TPPL from individual nanorods was collected by the same objective and focused either on a single-photon avalanche photodiode for imaging purposes or directed into a spectrograph [3]. All the spectra presented in this Letter were background corrected by offsetting the nanorods out of the confocal excitation. The TPPL yield was measured to be quasiquadratic with average excitation power. A fit to the data points reveals a slope of approximately 2.4, indicative of a two-photon process ruling out fourth order nonlinearity [11].

Figure 1(a) shows the normalized TPPL and scattering spectra of a series of single nanorods with differing aspect ratio r. The average excitation power P_{exc} was kept constant at 60 μW corresponding to a peak intensity of roughly 4 GW/cm^2 in the focus. The polarization was oriented along the longitudinal axis of the rods. The TPPL of the larger rods ($10 < r < 5$) shows an increased emission intensity towards the excitation wavelength sug-

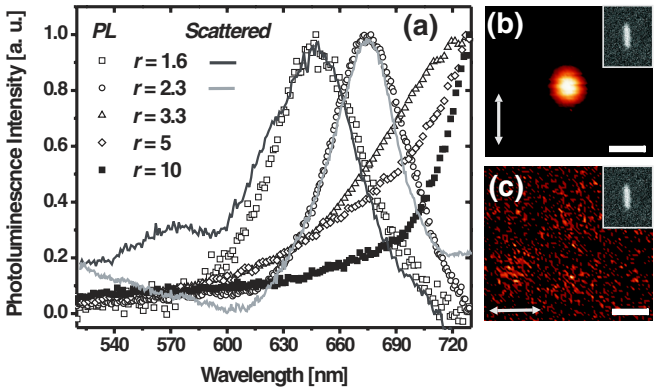

FIG. 1 (color online). (a) Two-photon induced photoluminescence spectra of gold nanorods with decreasing aspect ratio. The solid lines correspond to the scattering spectra for $r = 1.6$ and 2.3. (b),(c) Confocal TPPL image of $r = 3.3$ vertically oriented nanorod (see inset micrographs) integrated over the 400–700 nm spectral region for $P_{exc} = 60\ \mu$W and a polarization oriented with the longitudinal axis and the transverse axis, as indicated by the white arrows (scale bars: 300 nm).

gesting the presence of a peak in the near infrared region. Infrared photoemission was attributed to linear near-field optical intraband transitions [3]. Consequently, IR emission has different characteristics than two-photon excited TPPL and is beyond the scope of this study. For smaller r, the emission is composed of a single peak situated on the blue side of the excitation and does not resemble bulk TPPL [6]. Figure 1(a) reveals a significant blueshift of the TPPL peak position for decreasing aspect ratio, showing a trend that is well known for particle plasmons. Absorption measurements of colloidal gold nanorods showed analogous shifts of the longitudinal resonance mode for decreasing r [15,16]. We acquired scattering spectra of two individual nanorods ($r = 1.6$ and 2.3) by dark-field spectroscopy and compared them to the corresponding TPPL spectra as shown by the solid lines in Fig. 1(a). The scattering spectra overlap the TPPL spectra for the two nanorods. This offers a first indicator of the strong relationship between the photoluminescence and the surface plasmon peak.

To confirm this plasmon characteristic, we aligned the polarization with the minor axis of the nanorods to study the transverse resonance. Interestingly, we observed little or no TPPL for all the nanorods studied here. Figure 1(b) shows a confocal image of a rod ($r = 3.3$) for a polarization oriented with its main axis. The count rate is $\sim 1.2 \times 10^6$ counts/sec at its maximum for $P_{exc} = 60\ \mu$W. Figure 1(c) shows the same confocal area for a polarization aligned with the transverse axis and only a residual background noise ($\sim 4 \times 10^3$ counts/sec) dominates the image. Because of the increased confinement of the charges at the two extremities of a nanorod due to electromagnetic singularities, the magnitude of the longitudinal surface plasmon is typically much larger than its transverse counterpart and larger field enhancements are thus obtained [17]. For nonlinear responses such as TPPL, their sensitivity to the field strength plays a predominant role on TPPL yield. It is therefore not surprising to observe no, or very little, photoemission for a polarization aligned with the transverse axis. Furthermore, transverse resonances are typically situated in the 500–550 nm spectral region and are heavily damped due to linear interband absorption.

Another aspect characterizing localized surface plasmons is their spectral dependence on the morphology of the nanoparticles. It is well known, for instance, that the main resonances of spherical-shaped particles are blueshifted from longitudinal resonances occurring in nanorods [17]. To determine whether the TPPL follows also a similar behavior, we investigated TPPL spectra of a single nanorod undergoing laser-induced morphological modifications. Rod-to-sphere shape transformation of colloidal gold nanorods illuminated by femtosecond laser pulses has been reported in the past [18,19]. The reshaping is mainly governed by a photothermal effect where local melting occurs at defect sites and at the surface. Figs. 2(a) and 2(b) show the evolution of the TPPL spectral shape with increasing P_{exc} for a single nanorod ($r = 3.3$). An overall increase of the TPPL intensity is observed in Fig. 2(a) when P_{exc} increases from 200 to 350 μW. A shoulder centered around 650 nm becomes visible at these higher excitation powers and was previously ascribed to the increased density of states around the X point of the Brillouin zone for single-crystal nanorods [9]. The shoulder is better defined at 350 μW and at that point the effect is reversible. Figure 2(b) shows the normalized TPPL spectra of the same nanorod for increasing P_{exc}. Clearly, the TPPL spectra of Fig. 2(b) are drastically different from spectra of Fig. 2(a). They are now composed of a single peak located in the visible spectral region and an irreversible blueshift of the peak is observed when increasing the average excita-

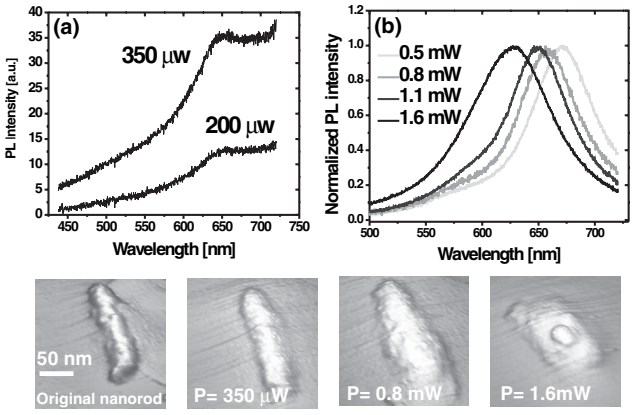

FIG. 2. (a) Modification of the TPPL spectral shape with increasing P_{exc} for a nanorod with $r = 3.3$. (b) Photoluminescence shift with increasing excitation power for the same nanorod indicating a morphological shape of the particle as shown in the series of AFM images.

tion power. An atomic force microscope (AFM) was used to image the morphology of the rod in the various irradiation stages as depicted in the series of three-dimensional images shown in the bottom of Fig. 2. The original topography of the rod (30 nm × 100 nm) is shown in the left-hand side picture. For $P_{exc} = 350$ μW, the dimension of the rod is not modified and only a smoother surface is observed indicative of a surface melting. The corresponding TPPL spectral characteristics [Fig. 2(a)] reflect only the result of the increased P_{exc}. For larger excitation power ($P_{exc} = 0.8$ mW), the shape of the rod starts to transform into a shorter and wider structure, consistent with laser-irradiated nanorods in solution [18]. The peaks of the TPPL blueshift with increasing power, strongly supporting the importance of the particle plasmon where longitudinal plasmon modes are known to blueshift with smaller aspect ratio [17]. For even larger power, the nanorod undergoes a drastic shape transformation into a thermodynamically favored nanodot [18] as shown by the right image at the bottom of Fig. 2. The particle's height changed from 45 nm for the original nanorod to 75 nm after the rod-to-dot transformation. While the original nanorod looks only partially melted and leftover material underneath the particle is still visible, the TPPL properties are dominated by the response of the quasispherical particle as discussed below.

For a particle with spherical symmetry, the plasmon resonance has an isotropic response to the polarization of the excitation field as opposed to a nanorod where longitudinal and transverse surface plasmons are polarization sensitive [17]. Consequently, if the TPPL properties follow the surface plasmon characteristics as indicated by Figs. 1 and 2, the TPPL yield of a spherical particle should also be isotropic with respect to the angle of the excitation field vector θ. Figure 3(a) shows a polar diagram of the normalized TPPL intensity emitted by a nanorod similar to the one studied above before (squares), during (triangles), and after (circles) laser-induced rod-to-dot transformation. The longitudinal axis of the nanorod corresponds to the vertical axis in Fig. 3(a). The polarization anisotropy ν defined as

$$\nu = \frac{I_{max} - I_{min}}{I_{max} + I_{min}} \quad (1)$$

is a good measure of the sensitivity to the polarization vector where I_{max} and I_{min} are the TPPL intensity for the polarization excitation oriented along the longitudinal and transverse axis, respectively. For the original, unmodified nanorod, the TPPL follows a $\cos^2\theta$ dependence [20] and ν is approximately 88%. For the wider and shorter modified nanorod, ν decreases to 84% as a result of the reduced aspect ratio. After shape transformation to the nanodot, the polarization anisotropy falls down to 55% indicating a TPPL response that is closer to the ideal isotropic characteristics of a spherical particle, consistent with the surface plasmon origin. After shape transformation, the direction

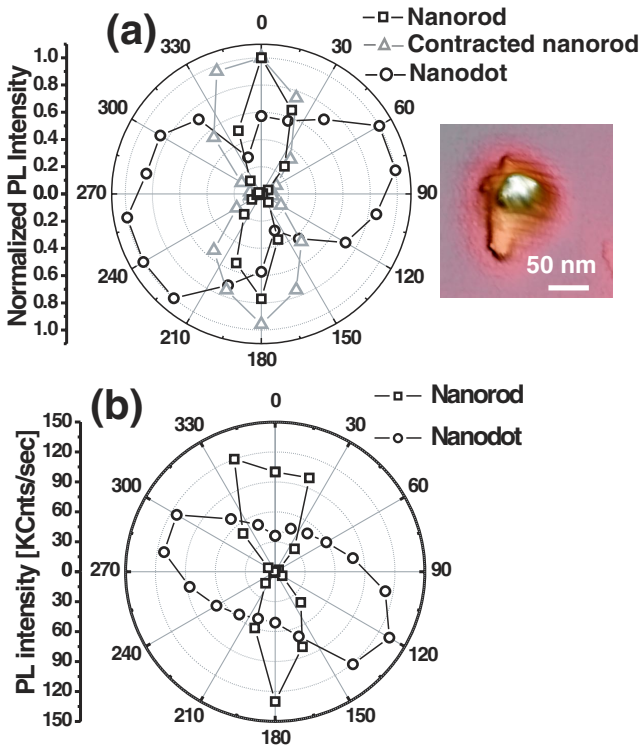

FIG. 3 (color online). (a) Normalized TPPL intensity (400–700 nm spectral region) as a function of the polarization orientation of the excitation field for the original nanorod (squares), modified rod (triangles), and nanodot (circles, and AFM image). (b) TPPL intensity from a nanorod (square) excited at 25 μW and its modified shape (circles) for an average power of 1.1 mW.

of I_{max} and I_{min} are rotated by ~80° due to a slight elongation of the transformed particle in a direction almost perpendicular to the incident polarization as shown in the AFM image in Fig. 3. We note that the underlying chromium adhesion layer of the original particle's shape is readily visible in the image and was not affected by the laser.

The TPPL yield is strongly influenced by the local field enhancement of the nanoparticle [3,10,11] and large field strength can be obtained by increasing the aspect ratio of ellipsoidal metal nanoparticles [17]. Consequently, in order to obtain a similar TPPL yield between a nanorod and a nanodot, the excitation power would have to be increased. Figure 3(b) shows the TPPL count rate as a function of polarization orientation of the excitation for a nanorod ($r = 3.3$) and its modified quasispherical particle. The polarization anisotropy is $\nu = 95\%$ and $\nu = 57\%$ for the rod and for the reshaped particle, respectively. The average laser power was increased from 50 μW for the nanorod to 1.1 mW for the transformed rod to obtain a comparable count rate (~130×10^6 counts/sec). At that point, it should be possible to estimate a relative enhancement factor difference between the two particles. However, while the TPPL yield follows a quadratic dependence for

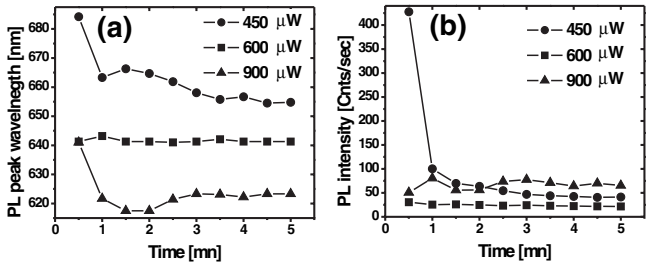

FIG. 4. (a) Spectral position of the TPPL peak for a 30 nm × 100 nm nanorod as a function of time for different average excitation powers. (b) Corresponding time dependence of the TPPL intensity.

low excitation power, the TPPL shows some instability in the count rate and has an erratic spectral position over relatively long time period at laser energies approaching the transformation threshold of the particle. The rod-to-sphere transformation is a fast process occurring within about 30 ps [21]. However, in our experiment the particles were exposed over a much longer time period (seconds to minutes) and dynamic effects of the shape transformation therefore influence the response of the particle. Figs. 4(a) and 4(b) show the temporal instability of the spectral maximum and count rate of the TPPL, respectively, from a 30 nm × 100 nm nanorod, with P_{exc} above the reshaping threshold. The nanorod was excited continuously for 5 min, and each data point corresponds to an integration time of 30 s. The position of the peak blueshifts with time for a fixed P_{exc} emphasizing the dynamic reshaping of the nanorod. The intensity for $P_{\mathrm{exc}} = 450\ \mu$W drastically drops after the second acquisition [Fig. 4(b)] indicating a decreased field enhancement. This is consistent with a reduced aspect ratio of the nanorod shown by the blueshift of the spectral peak in Fig. 4(a). For subsequent $P_{\mathrm{exc}} = 600\ \mu$W, both peak position and intensity are relatively stable in time indicating a stabilized shape of the nanoparticle. For subsequent higher excitation power of the same particle, the peak position continues to blueshift and shows large spectral instability and the TPPL intensity slightly oscillates. The TPPL magnitude is drastically reduced compared to the TPPL intensity emitted from the original nanorod despite the increased P_{exc} as a consequence of the lower field enhancement.

In summary, we have shown that two-photon excited gold photoluminescence emitted by individual nanorods and nanodots is correlated with localized surface plasmons and have the same optical characteristics. In particular, we demonstrated experimentally that the spectral position of the TPPL blueshifts with decreasing aspect ratio and observed a shape-dependent TPPL spectra upon laser-induced rod-to-dot transformation. These behaviors are consistent with the properties of localized surface plasmon resonances and offer a way to optically control and produce selected emission wavelengths from a single nanoparticle. The TPPL yield is characterized by a polarization anisotropy that changes during the different structural phases of the reshaping process. As a consequence of the underlying influence of the plasmon resonance on the local field strength, the photoluminescence yield of the nanorod is drastically reduced after reshaping. TPPL can also be considered as a background-free means to detect the plasmon shifts of metal nanoparticles in response to different dielectric media or molecular adsorbates, thereby providing improved sensor capabilities and addressable modulation of photoluminescence.

The authors thank M. Beversluis and J. J. Greffet for discussions. This work was supported by the U.S. Department of Energy, Basic Energy Science-Materials Sciences, under Contract No. W-31-109-ENG-38, the Conseil Régional de Champagne-Ardennes, and the European Social Funds.

[1] C. K. Chen, A. R. B. de Castro, and Y. R. Shen, Phys. Rev. Lett. **46**, 145 (1981).
[2] G. T. Boyd, Z. H. Yu, and Y. R. Shen, Phys. Rev. B **33**, 7923 (1986).
[3] M. R. Beversluis, A. Bouhelier, and L. Novotny, Phys. Rev. B **68**, 115433 (2003).
[4] V. A. Markel *et al.*, Phys. Rev. B **59**, 10 903 (1999).
[5] A. M. Michaels, J. Jiang, and L. Brus, J. Phys. Chem. B **104**, 11 965 (2000).
[6] A. Mooradian, Phys. Rev. Lett. **22**, 185 (1969).
[7] R. A. Farrer, F. L. Butterfield, V. W. Chen, and J. T. Fourkas, Nano Lett. **5**, 1139 (2005).
[8] A. Bouhelier, M. R. Beversluis, and L. Novotny, Appl. Phys. Lett. **83**, 5041 (2003).
[9] K. Imura, T. Nagahara, and H. Okamoto, J. Am. Chem. Soc. **126**, 12 730 (2004).
[10] P. J. Schuck *et al.*, Phys. Rev. Lett. **94**, 017402 (2005).
[11] P. Mühlschlegel, H.-J. Eisler, O. J. F. Martin, B. Hecht, and D. W. Pohl, Science **308**, 1607 (2005).
[12] D. J. Roaf, Phil. Trans. R. Soc. A **255**, 135 (1962).
[13] M. B. Mohamed *et al.*, Chem. Phys. Lett. **317**, 517 (2000).
[14] E. Dulkeith *et al.*, Phys. Rev. B **70**, 205424 (2004).
[15] S. Link, B. Mohamed, and M. A. El-Sayed, J. Phys. Chem. B **103**, 3073 (1999).
[16] N. R. Jana, L. Gearheart, and C. J. Murphy, Adv. Mater. **13**, 1389 (2001).
[17] U. Kreibig and M. Vollmer, *Optical Properties of Metal Clusters* (Springler-Verlag, Berlin, 1994).
[18] S. Link, C. Burda, B. Nikoobakht, and M. A. El-Sayed, J. Phys. Chem. B **104**, 6152 (2000).
[19] S. Link, Z. L. Wang, and M. A. El-Sayed, J. Phys. Chem. B **104**, 7867 (2000).
[20] K. Imura, T. Nagahara, and H. Okamoto, J. Phys. Chem. B **109**, 13 214 (2005).
[21] S. Link, C. Burda, B. Nikoobakht, and M. A. El-Sayed, Chem. Phys. Lett. **315**, 12 (1999).